



Application of CAD Analysis to Update the Design for a Pectus Excavatum Bar Extraction Tool

Krzysztof J. Rechowicz¹, Frederic D. McKenzie¹, Sebastian Y. Bawab² and Robert Obermeyer³

¹Old Dominion University, krech001@odmckenz.odu.edu

²Old Dominion University, sbawab@odu.edu

³Children's Hospital of The King's Daughters, robert.obermeyer@chkd.org

ABSTRACT

The Nuss procedure is a minimally invasive procedure for the correction of pectus excavatum - a chest wall deformity which results in the placement of a metal bar inside the chest cavity. The bar is removed after approximately two years. Surgeons have been reporting that the currently available tools for the extraction of the bar do not provide the most optimal functionality. Previously, we had proposed a novel design of the tool which showed deficiencies when experimentally tested. With the aid of CAD and finite element analysis, modifications to the original design were adopted to drastically increase the factor of safety. The improved tool is prototyped and will be clinically evaluated by the surgeon.

Keywords: CAD, finite element analysis, surgical tools, Nuss procedure.

DOI: 10.3722/cadaps.2012.227-234

1 INTRODUCTION

Pectus excavatum (PE), also called sunken or funnel chest, is a congenital chest wall deformity which is characterized, in most cases, by a deep depression of the sternum (fig. 1). This condition affects primarily children and young adults and is responsible for about 90% of congenital chest wall abnormalities [1]. Typically, this deformity can be found in approximately one in every 400 births and is inherited in many instances [2]. Among various PE treatment options, the minimally invasive technique for the repair of PE, often referred to as the Nuss procedure, has been proven to have a high success rate, satisfactory aesthetic outcome and low interference with skeletal growth [2].

The Nuss procedure involves placing a metal bar(s) (fig. 2) underneath the sternum forcibly changing the geometry of the ribcage. Apart from a physical improvement, positive psychological results are attributed to surgical correction [3, 4] because the normal shape of the chest is restored, reducing embarrassment, social anxiety, and depression [5].



Fig. 1: Photo of male with PE.



Fig. 2: Pectus bar.

The pectus bar removal process starts with making incisions in the side of the torso in the same locations as the ones made during the implantation. The curvature of the bar does not allow for direct removal. To overcome this difficulty, a pair of tools for pectus bar removal, called benders by the manufacturer, are used to firstly straighten the bar. Surgeons identify two problems associated with using these tools. First, significant length of the bar has to be exposed to place the tool in such a way to provide a counterforce. Second, engagement of the other tool with the end of the bar can be obstructed by tissue growth.

Motivated by those issues, we had previously designed, using a CAD software, an optimized surgical tool for the pectus bar extraction and performed finite element analysis (FEA) to validate our approach (fig. 3). Additionally, physical models and metal prototypes of the tool were built in order to allow evaluation of various design variants by the potential end users - the surgeons from the Children's Hospital of the King's Daughters, where the Nuss procedure was developed.

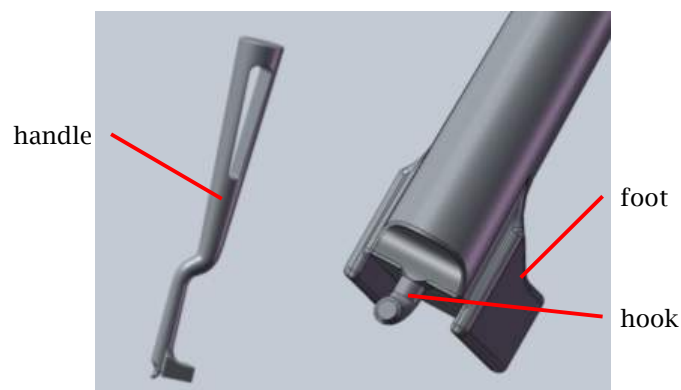


Fig. 3: Final design: whole tool (left), hook and lever arm (right).

However, the metal prototypes failed during our initial testing. The hook in the lower part of the tool changed its curvature making further use dangerous and not possible. In this paper, we present an approach to identify and solve causes of the failure. We utilized CAD models to study the interaction of the tool with a pectus bar and based on resulting observations we updated the initial design. Then, FEA was performed to identify stress magnitude and distribution in the hook. Based on the updated design, we manufactured metal prototypes which passed our initial testing and will be submitted for clinical testing by the projects surgeon collaborator.

2 METHODOLOGY

2.1 Probable Causes of Failure

The initial design assumed the use of AISI 304 half hard stainless steel resulting in a factor of safety of 1.42 in the direction of the highest stress. However, steel used to manufacture the metal prototype was not treated thermally.

Since the hook in the metal prototype was welded in, we expected that heat from the process could alter mechanical properties. We measured hardness of the original material used for the hook and thermally treated it similarly to welding. There was a decrease in hardness where heat was applied, but outside that region changes were negligible. The region just outside the heated part of the hook was the region of interest. Therefore, it cannot be assumed that heat was a main cause of failure, but it could contribute to further decrease of the factor of safety.

Suboptimal diameter of the hook can be considered as another cause of failure. Since the diameter is relatively small, even slight changes in that dimension can lead to drastical changes in stress. Moreover, as reported by surgeons, and opposite to our initial assumption, the end of a pectus bar has minimal curvature which leads to a situation where the foot reaction force is close to midspan (distance a rather than c) as illustrated in fig. 4. Therefore, decreasing that distance from value a to c , where $a > c$, will drastically increase the force F leading to higher stresses. This was one of the biggest factors to drop our factor of safety in our first prototype as compared with our initial design.

To validate our assumption, the original model was modified accordingly where diameter of the hook was 3.3 mm and the distance was approximately 15 mm, the equivalent force F applied to the hook was 1418 N, the yield strength of the material according to the supplier was 620 MPa.

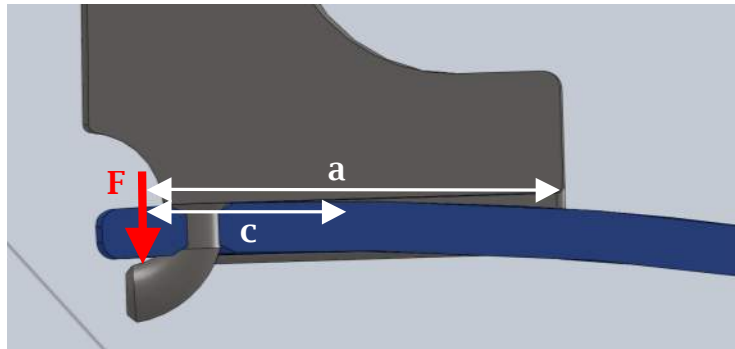


Fig. 4: The initial design of the tool engaged with the bar.

Fig. 5 left shows that von Mises stress for the red area is 2034 MPa and fig. 5 right shows that in the y -direction stress for the red area 2153 MPa. These lead to a factor of safety 0.3 and 0.28, respectively. These show that an updated design is necessary and, as our initial calculations showed, possible.

Based on those observations, we decided to employ CAD software to find possible ways to improve the strength of the tool within the constraints imposed by potential users.

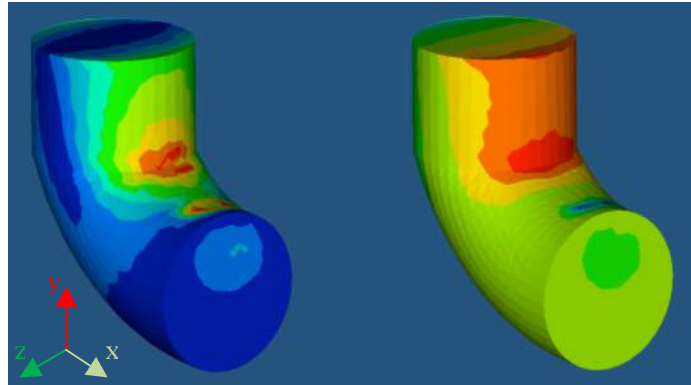


Fig. 5: Distribution of stress in the initial design: von Mises (left), y-direction (right).

2.2 Updated Design

A 3D model of the updated tool was developed in SolidWorks (Dassault Systems, MA, USA). To overcome the first problem, posed by curvature of the bar, we decided to place a step at the end of the foot (fig. 6) which will ensure that the longest possible distance is used. Moreover, we extended the length of the foot from 22 to 27 mm in order to decrease forces acting on the hook. This distance is crucial in terms of the benefits provided by our tool. The longer the distance, the more of the bar needs to be exposed by larger incisions on the side of the patient. However, after consultation with surgeons, adding 5 mm would not violate this constraint, since typically an incision from 30 to 40 mm is made.

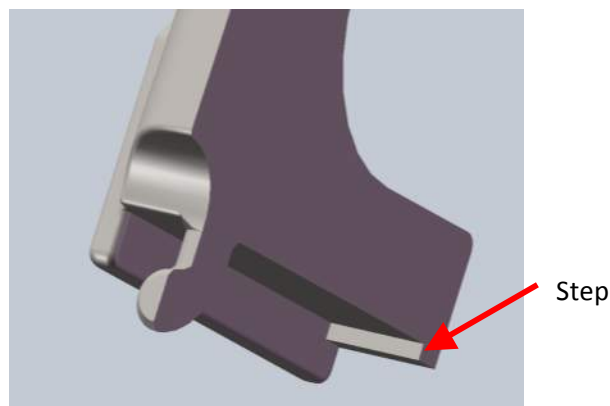


Fig. 6: The step at the end of the foot.

To further increase strength of the tool, we decided to maximize the diameter of the hook, because even its slight increase can lead to significant improvement since stress is reversely proportional to a cross section. However, in order to correctly engage the tool with the bar, the hook diameter cannot be directly determined by the size of the hole in a pectus bar.

To find the optimal diameter of the hook, we gradually increased its size and performed simulation in the CAD environment of the tool-bar engagement with collision detection turned on (fig. 7). If the hook could not be introduced, a collision detection would be signaled. Using this approach, we were able to increase the area of a hook cross section by 30%.

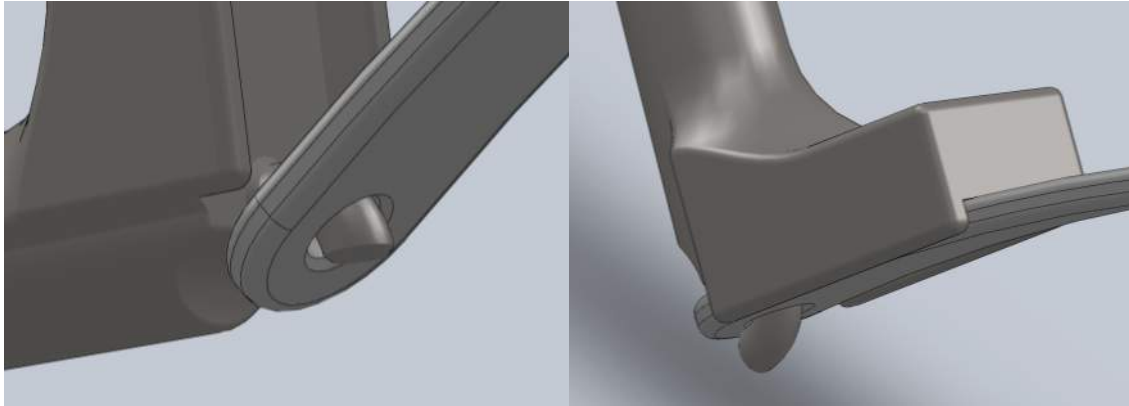


Fig. 7: Tool-bar engagement simulation: the beginning (left), final position (right).

The last improvement is related to the material used for the hook. Instead of using grade 300 stainless steel, we utilized 17-4 H900 stainless steel. In this way, yield strength was increased by 68%. The remaining part of the tool can be manufactured using a lower grade steel since it carries much lower loads than the hook.

2.3 Finite Element Analysis

Since this is a surgical tool, the safety of our design must be ensured. We performed FEA simulating the straightening process, but we focused only on the hook since we already know that stresses in the remaining part of the tool are significantly smaller.

A 3D model of the hook, after removing unnecessary features (fig. 8 left), like fillets and chamfers, was converted to IGES format to provide the best interoperability with FEA preprocessor - HyperMesh (Altair, MI, USA). Radioss (Altair) was utilized as the FE solver. A solid model of the hook was converted to a FE model containing 9188 tetrahedral elements. This procedure allowed us to save time needed for computations and reduced risk of errors during import to the FEA environment.

The new tool clearly identifies that a 133 N force applied to the handle results in a total force of 820 N applied on the top of the hook (fig. 8 right). This force is linearly distributed over four nodes.

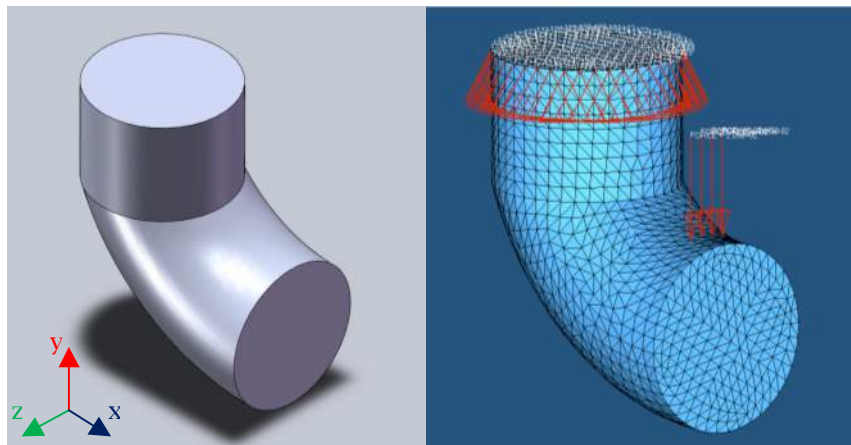


Fig. 8: The hook: CAD model (left), FE model with constraints and forces (right).

We assumed stainless steel 17-4 H900 as the material for the hook. In this case modulus of elasticity is 207 GPa and yield strength is 1275 MPa. For the metal prototype, we assumed stainless steel 304 with the same modulus of elasticity and yield strength of 758 MPa.

Fig. 9 depicts von Mises stresses in the hook. The red area corresponds to 913 MPa, whereas the orange to 813 MPa. These result in a factor of safety equal to 1.4 for the red area and 1.57 for the orange area.

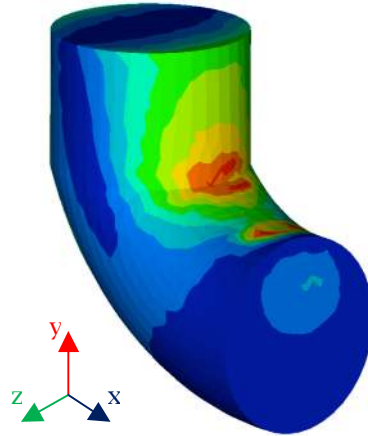


Fig. 9: Distribution of von Mises stress in the hook.

However, the largest stress had been expected along the y -direction of forces acting on the hook. According to fig. 10, the red area corresponds to 967 MPa and the orange area to 700 MPa. These result in a factor of safety 1.32 for the red area and 1.82 for the orange area.

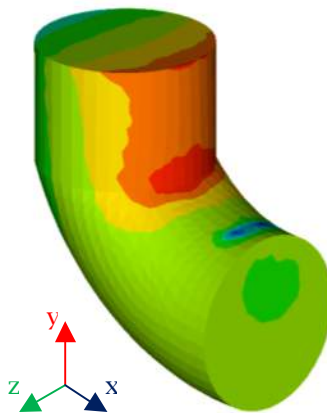


Fig. 10: Stress pattern along the y -direction.

For the x (fig. 11) and z -direction (fig. 12) the stresses are significantly smaller - 570 MPa and 290 MPa, respectively. These results have a factor of safety 2.24 for the x -direction and 4.4 for the z -direction. A factor of safety above 1 indicates that the material and design are adequate.

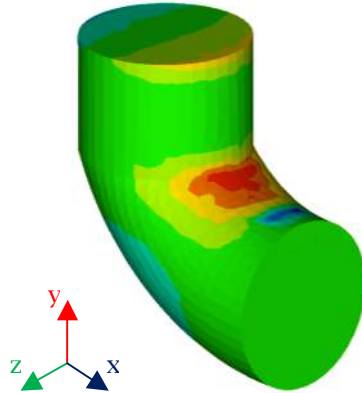


Fig. 11: Stress pattern along the x -direction.

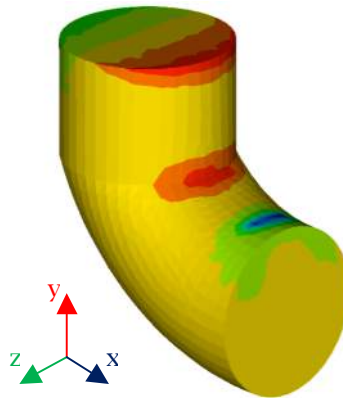


Fig. 12: Stress pattern along the z -direction.

2.4 Metal Prototype

Based on the results of the simulation performed in the CAD system, the FEA, and the previously developed physical models [6], we manufactured metal prototypes of the tool (fig. 13 left) and tested them by straightening pectus bars (fig. 13 right). Visual inspection of the hook after multiple straightening trials in a laboratory environment did not reveal any deformities.



Fig. 13: Metal prototype of the updated design: the hook and the foot (left), engagement with the pectus bar (right).

3 CONCLUSIONS

Motivated by the issues reported by the surgeons from the CHKD regarding the optimized tool for pectus bar extraction, we employed an iterative method of applying CAD tools, FEA software and manufacturing of first conceptual models and then metal prototypes to update initial designs of the tool. By using this approach, we were able to overcome reported issues and, at the same time, maintain advantages that make our tool superior to the commercial bar benders currently being used in terms of shortening the time of surgery which limits costs and reduces the risk of infection. Additionally, FEA proved that the updated design provides safety, because all factors of safety are above 1, and strength to withstand the stresses present in the bar straightening process.

In the next and final step, the metal prototypes will be used by surgeons from the CHKD in a clinical study to evaluate the actual bar removal procedure on patients. This will ultimately prove the adequacy of the design presented in this paper.

REFERENCES

- [1] Pretorius, S.E.; Haller, A.J.; Fishman, E.K.: Spiral CT with 3D Reconstruction in Children Requiring Reoperation for Failure of Chest Wall Growth after Pectus Excavatum Surgery, *Clinical Imaging*, 22(2), 1998, 108-116, DOI:10.1016/S0899-7071(97)00073-9
- [2] Protopapas, A. D.; Athanasiou, T.: Peri-operative data on the Nuss procedure in children with pectus excavatum: independent survey of the first 20 years' data, *Journal of Cardiothoracic Surgery*, 40(3), 2008, DOI:10.1186/1749-8090-3-40
- [3] Krasopoulos, G.; Dusmet, M.; Ladas, G. ; Goldstraw, P.: Nuss procedure improves the quality of life in young male adults with pectus excavatum deformity, *European Journal of Cardiothoracic Surgery*, 29, 2006, 1-5, DOI:10.1016/j.ejcts.2005.09.018
- [4] Lawson, M. L.; Cash, T. F.; Akers, R.; Vasser, E.; Burke, B.; Tabangin, M.; Welch, C.; Croitoru, D. P.; Goretsky, M. J.; Nuss, D.; Kelly Jr., R. E.: A pilot study of the impact of surgical repair on disease-specific quality of life among patients with pectus excavatum, *Journal of Pediatric Surgery*, 38(6), 2003, 916-918, DOI:10.1016/S0022-3468(03)00123-4
- [5] Einsiedel E.; Clausner, A.: Funnel chest. Psychological and psychosomatic aspects in children, youngsters, and young adults, *Journal of Cardiovascular Surgery*, 40(5), 1999, 733-736.
- [6] Rechowicz, K.J.; McKenzie, F.D.; Bawab, S.Y.; Obermeyer, R.: Optimized surgical tool for pectus bar extraction, in *Engineering in Medicine and Biology Society (EMBC), 2010 Annual International Conference of the IEEE*, 2010, 1254-1257, DOI:10.1109/IEMBS.2010.5626425